A Polymer-Bound Oxidovanadium(IV) Complex Prepared from an L-Cysteine-Derived Ligand for the Oxidative Amination of Styrene

Mannar R. Maurya,*[a] U. Kumar,[a] Isabel Correia,[b] Pedro Adão,[b] and João Costa Pessoa[b]
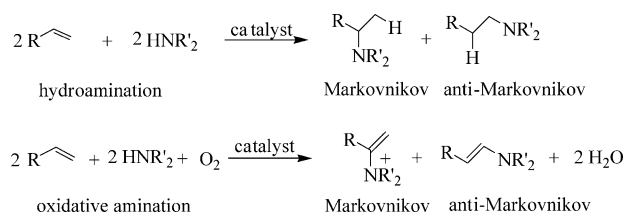
The ligand H_2sal-cys (**I**) derived from salicylaldehyde and L-cysteine has been covalently bonded to chloromethylated polystyrene cross-linked with 5 % divinylbenzene. Upon treatment with [VO(acac)$_2$] in dimethylformamide (DMF) the polystyrene-bound ligand PS-H_2sal-cys (**II**) gave the oxidovanadium(IV) complex, PS-[VO(sal-cys)·DMF] (**1**). The corresponding neat complex, [VO(sal-eta)]$_2$ (**2**), has also been prepared similarly in methanol. These complexes have been characterised by IR, electronic, EPR spectroscopic studies, magnetic susceptibility measurements and thermal as well as scanning electron micrographs studies. Complex [VO-(sal-eta)]$_2$ exhibits a medium intensity band at 980 cm^{-1} in the IR spectrum due to ν(V=O) stretch. Broad features of the EPR spectrum for the neat complex along with magnetic susceptibility studies suggest the presence of antiferromagnetic exchange interaction between two vanadium centers in close proximity. Both complexes catalyze the oxidative amination of styrene, in mild basic conditions, with secondary amines (diethylamine, imidazole, and benzimidazole) and gave a mixture of two aminated products in good yields. Amongst the two aminated products, the anti-Markovnikov product is favored over the Markovnikov one due to the steric hindrance posed by the secondary amines. The polymer-anchored heterogeneous catalyst is free from leaching during catalytic action and recyclable.

(© Wiley-VCH Verlag GmbH & Co. KGaA, 69451 Weinheim, Germany, 2008)

Introduction

Metal-catalyzed addition of nucleophilic amines to alkenes, called amination, represents one of the important routes to synthesize nitrogen-based organic molecules.[1] The amination may proceed in the presence or absence of oxygen and the processes, called oxidative amination or hydroamination, respectively, are both highly useful. On the basis of regioselectivity, Markovnikov or anti-Markovnikov products may be produced (Scheme 1).
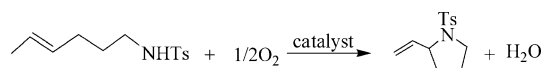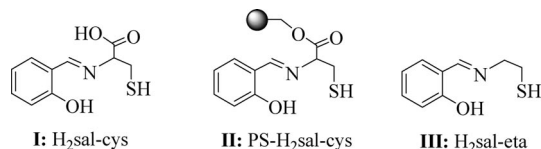
Scheme 1.

Nonactivated alkenes are generally resistant toward nucleophilic attack of amines, but upon complexation to an electrophilic transition metal, olefins become susceptible toward nucleophiles.[1] The subsequent addition of the amine depends on the steric nature of the olefin and amine. The nucleophilic nitrogen normally reacts in such a way that the least-hindered metal alkyl complex is formed (Markovnikov addition), but steric factors of the amine substituents may dominate the reaction favoring the anti-Markovnikov products.[1]

Catalytic intramolecular amination of alkenes may also result if a secondary amine group is present on the alkene itself at an appropriate position (e.g. Scheme 2). Efficient catalytic intramolecular hydroamination of alkenes has also been developed.[1–7] Normally catalysts based on late transition-metal complexes (e.g. of Pd, Pt, Ru, Rh etc.) or lanthanides are used for aminations. Though these complexes are less sensitive towards oxygen, literature cites reports on hydroamination[1–7] as well as oxidative aminations.[8–21] Since complexes of early transition metals, e.g. vanadium, are frequently used as oxidation catalysts, they are potential candidates for oxidative aminations. However, no oxidative amination using vanadium complexes as catalysts has been reported in the literature. We, therefore, decided to prepare oxidovanadium(IV) complexes and use them as catalysts for the oxidative amination of styrene.

[a] Department of Chemistry, Indian Institute of Technology Roorkee,
    Roorkee 247667, India
    E. mail: rkmanfcy@iitr.ernet.in
[b] Centro Química Estrutural, Instituto Superior Técnico – TU Lisbon,
    Av. Rovisco Pais, 1049-001, Lisboa, Portugal

M. R. Maurya, U. Kumar, I. Correia, P. Adão, J. Costa Pessoa

Scheme 2.

Scheme 4. Synthetic procedure for **II**. PS represents the polystyrene support.

In this work the synthesis and characterization of a polymer-anchored oxidovanadium(IV) complex of the Schiff base derived from salicylaldehyde and cysteine [H₂sal-cys **I**; Scheme 3] is reported. We demonstrate the catalytic performance of the complex, PS-[VO(sal-cys)·DMF] (**1**) [PS-H₂sal-cys (**II**), PS = polystyrene backbone; Scheme 3] in the oxidative amination of styrene with secondary amines such as diethylamine, imidazole, and benzimidazole in mild basic conditions. Covalent bonding to polystyrene provides extra stability to the catalyst and makes the catalytic reaction heterogeneous in nature. The neat complex [VO(sal-eta)]₂ [H₂sal-eta (**III**) is the Schiff base derived from salicylaldehyde and 2-aminoethanethiol; Scheme 3] having similar donor atoms has also been prepared and its catalytic activity is compared with that of the polymer-anchored complex.

The anchored ligand, PS-H₂sal-cys reacts with [VO(acac)₂] in DMF at ca. 90 °C to give the polymer-anchored blackish green oxidovanadium(IV) complex, PS-[VO(sal-cys)·DMF] (**1**); Scheme 5.

Scheme 5. Synthetic procedure for **1**.

Similarly, the reaction of [VO(acac)₂] with an equimolar amount of neat ligand, H₂sal-eta (**III**), in refluxing acetonitrile yielded the neat oxidovanadium(IV) complex, [VO(sal-eta)]₂ (**2**); see Equation (1).

$$[VO(acac)_2] + H_2sal\text{-}eta \rightarrow \frac{1}{2}[VO(sal\text{-}eta)]_2 + 2\ Hacac$$

$$\mathbf{2}$$

(1)

Scheme 3.

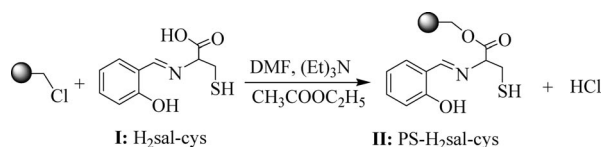## Results and Discussion

Synthesis, Solid-State Characterization, and Reactivity

The elemental analyses data of the ligands and complexes are presented in Table 1. The spectroscopic characterization (IR, ¹H and ¹³C NMR) of the ligands, H₂sal-cys (**I**) and H₂sal-eta (**III**), used in the present study, confirm their structure. The chloromethylated polystyrene, cross-linked with 5% divinylbenzene, reacts with H₂sal-cys in DMF in the presence of triethylamine and ethyl acetate to give the polymer-anchored ligand PS-H₂sal-cys (**II**). Scheme 4 summarizes the synthetic procedure. During this process the –COOH group of cysteine reacts with the –CH₂Cl group of polystyrene. The remaining chlorine content of 1.6% (0.46 mmol Cl g⁻¹ of resin in PS-H₂sal-cys) suggests ca. 91% loading of the ligand.
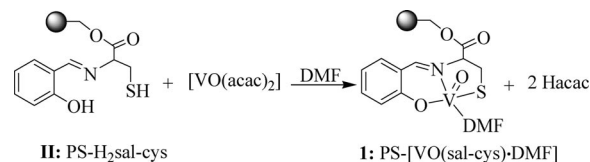
Complex **2** exhibits an effective magnetic moment of 1.47 μ_B at 298 K, which is subnormal compared with the expected value of 1.73 μ_B for d^1($S = \frac{1}{2}$) systems. We have also studied the magnetic susceptibility of the complex as a function of temperature in the 90–298 K range. Figure 1 presents the plots of magnetic moment (μ_B) and magnetic susceptibility (χ_M^{corr}) vs. temperature for **2**. The χ_M^{corr} shows a slight dependence on temperature and the observed magnetic moments vary in the range 1.47–1.19 μ_B. The Curie–Weiss plot [$1/\chi_M^{corr}$ vs. T] shown in Figure 2 is a straight line with a Weiss constant of –60 K. These results indicate an antiferromagnetic interaction, probably due to a dimeric

Table 1. Physico-chemical data of the solid compounds.

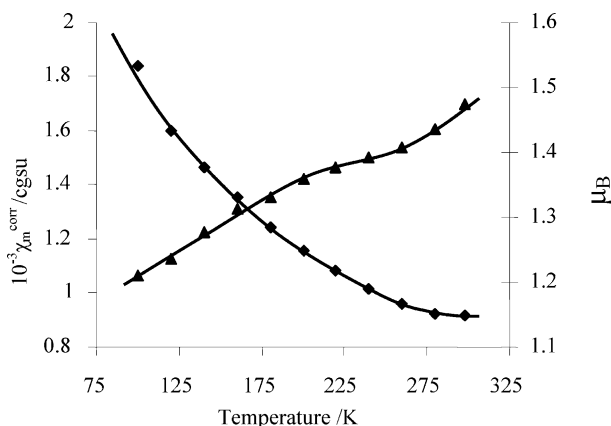| Compound	Color	Observed[a] (%)				
		C	H	N	S	V
PS-H₂sal-cys (**II**)	orange	72.59	8.14	3.56	5.96	–
PS-[VO(sal-cys)·DMF] (**1**)	blackish green	68.78	7.82	4.01	5.40	8.01
H₂sal-eta (**III**)	yellow	60.23	6.25	7.63	17.18	–
		(59.66)	(6.07)	(7.73)	(17.67)	
[VO(sal-eta)]₂ (**2**)	green	44.31	3.94	5.64	12.81	20.0
		(43.90)	(3.65)	(5.69)	(13.00)	(20.73)

[a] Calculated values for neat ligand and complex are given in parenthesis.

Figure 1. Plot of the magnetic moment (μ_B) and magnetic susceptibility (χ_m^{corr}) vs. temperature for [VO(sal-eta)]₂ (**2**).

structure of the complex. Syamal and Kale[22,23] have suggested an antiferromagnetic interaction through dimerization in the related complex [VO(sal-ea)]$_2$ (H$_2$sal-ea is the Schiff base derived from salicylaldehyde and 2-aminoethanol) based on the magnetic susceptibility data and EPR studies, and later confirmed by a single-crystal X-ray diffraction study.[24] We have also previously observed dimerization of [VO(sal-ohyba)] (H$_2$sal-ohyba is the Schiff base derived from salicylaldehyde and *o*-hydroxylbenzylamine).[25]
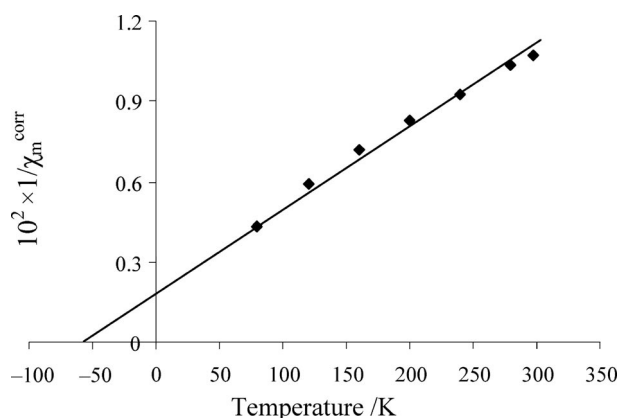

Figure 2. Curie–Weiss plot [1/χ_m^{corr} vs. *T*] for [VO(sal-eta)]$_2$ (2).

Scanning Electron Micrograph Study

Scanning Electron Micrographs (SEM) for single beads of pure chloromethylated polystyrene, PS-H$_2$sal-cys (II) and PS-[VO(sal-cys)·DMF] (1) were obtained to observe the morphological changes. Images of II and 1 are reproduced in Figure 3. As expected, the pure polystyrene bead has a smooth and flat surface, while the anchored ligand and complex show slight roughening of the top layer. This roughening is more intense in 1 possibly due to the interaction of vanadium with the anchored ligand that results in
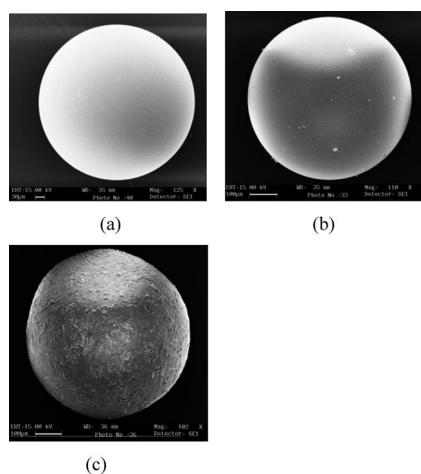

Figure 3. Scanning electron micrographs (SEM) of (a) PS-H$_2$sal-cys (II), (b) PS-[VO(sal-cys)·DMF] (1), and (c) PS-[VO(sal-cys)·DMF] (1) (after swelling); magnification ca. 200.

the formation of a complex with fixed geometry. Because of poor loading of the metal complex it was not possible to obtain accurate information on the morphological changes in terms of orientation of ligands coordinated to the metal ion. A scanning electron micrograph of complex 1 after keeping it in acetonitrile for 2 h has also been recorded and is reproduced in Figure 3(c). Upon swelling the beads the opening of the pores can be visualized.

TGA Study

Thermogravimetric analysis under an oxygen atmosphere show the high stability of PS-[VO(sal-cys)·DMF] (1) up to ca. 175 °C. The first weight loss starting just above 175 °C is possibly due to coordinated DMF. Thereafter the complex decomposes in several steps. Quantitative measurement of weight loss at various stages was not possible due to their overlap. However, the stability of final residues at ca. 700 °C suggests the formation of V$_2$O$_5$. The metal content calculated from the final residues was close to the one obtained by atomic absorption spectrometry.

IR Spectral Study

A partial list of selected IR absorption bands of ligands and complexes is given in Table 2. The absence of peaks at 1264 and 673 cm^{-1} due to the –CH$_2$Cl group of chloromethylated polystyrene in the polymer-anchored ligand suggests the covalent bonding of chloromethylated polystyrene to the ligand.[26] A sharp band due to ν(C=O) of carboxylate appears at ca. 1665 cm^{-1} in the polymer-anchored ligand and complex. The ν(C=N) (azomethine) stretch of PS-H$_2$sal-cys shows up at 1632 cm^{-1}. This peak shifts to lower wave numbers upon coordination (1619 cm^{-1}) indicating the coordination of the azomethine nitrogen atom. Similarly, III exhibits this band at 1632 cm^{-1}, which is shifted to 1620 cm^{-1} in 2. The coordination of the phenolic oxygen atom is indicated by the absence of the band centered at ca. 3400 cm^{-1} in the complexes. It was not possible to identify bands confirming the coordination of DMF in 1 due to the strong absorption of ν(C=O) in the same region. Both complexes also exhibit sharp strong bands at 980 cm^{-1} due to ν(V=O).

Table 2. Selected IR spectroscopic data (wavenumbers, cm^{-1}).[a]

Compound	ν(OH)	ν(C=N)	ν(V=O)
PS-H$_2$sal-cys (II)	3400 (br)	1632	–
PS-[VO(sal-cys)·DMF] (1)	–	1619	980 (sh, s)
H$_2$sal-eta (III)	3400 (br)	1632	–
[VO(sal-eta)]$_2$ (2)	–	1620	980 (sh, s)

[a] br = broad, sh = sharp, s = strong.

UV/Vis Spectroscopic Studies

As expected, broader bands are observed in the case of the polymer-anchored complex in nujol as compared to the

neat complex, and some relevant data are presented in Table 3. The electronic spectrum of H$_2$sal-eta (**III**) in methanol exhibits three UV bands at 215, 255, and 316 nm. These bands are assigned to $\phi\rightarrow\phi^*$, $\pi\rightarrow\pi^*$, and $n\rightarrow\pi^*$ transitions, respectively. The band at 253 nm is also observed in the spectrum of [VO(sal-eta)]$_2$ (**2**), but the 215 nm band could not be located. The broad transition at ca. 350 nm in complex **2** is possibly due to merging of a LMCT band with the $n\rightarrow\pi^*$ intraligand band. In addition, **2** in DMF displays two weak broad bands at 536 and 605 nm due to d–d transitions, confirming the presence of a vanadium(IV) center. The polymer-anchored ligand PS-H$_2$sal-cys (**II**) in nujol is similar to that of **III**, with only slight deviation in their positions (Figure 4). Complex PS-[VO(sal-cys)·DMF] exhibits a broad featured band at 395 nm possibly due to a LMCT band in addition to the other three intraligand bands.

Table 3. Electronic spectra of ligands and complexes.

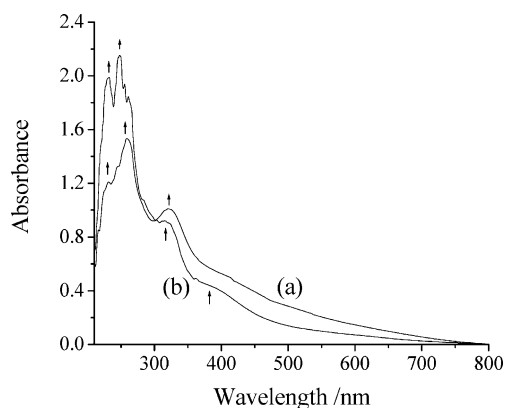| Compound	Solvent	λ_{max} [nm]
H$_2$sal-eta	acetonitrile	316, 255, 215
H$_2$sal-cys	acetonitrile	350, 272, 218
[VO(sal-eta)]$_2$	dichloromethane	605, 535, 350, 253
PS-H$_2$sal-cys	nujol	323, 260, 231
PS-[VO(sal-cys)·DMF]	nujol	395, 321, 242, 230

Figure 4. Electronic spectra of (a) PS-(H$_2$sal-cys) (**II**) and (b) PS-[VO(sal-cys)·DMF] (**1**) recorded in nujol.

EPR Spectroscopic Study

The EPR spectra of samples of the neat and polymer-anchored complexes were obtained from "frozen" solutions (77 K) and powder, respectively. The anisotropy is not totally averaged away by motion of the molecules and nearly axial EPR spectra were obtained.

After carrying out the catalytic reactions the polymer-anchored catalyst **1** was filtered, washed and dried, and its EPR spectrum was recorded under the same conditions as that of the freshly prepared PS complex. Both spectra are shown in Figure 5. The spectra of the fresh and spent catalyst are identical indicating that the environment and coordination geometry of the vanadyl ion were retained after the catalytic reaction. Both spectra are characteristic of

magnetically diluted V^{IV}O complexes and show a slight rhombic distortion, which can be seen in the perpendicular lines M_I = 7/2 and 5/2, indicating a small distortion of the square pyramidal geometry. The resolved EPR pattern indicates that the vanadium centers are well dispersed in the polymer matrix. The spectra were simulated and the spin Hamiltonian parameters obtained are $g_x = 1.980$, $g_y = 1.975$, $g_z = 1.938$, $A_x = 63.1\times10^{-4}$ cm^{-1}, $A_y = 66.5\times10^{-4}$ cm^{-1}, $A_z = 173.3\times10^{-4}$ cm^{-1}.
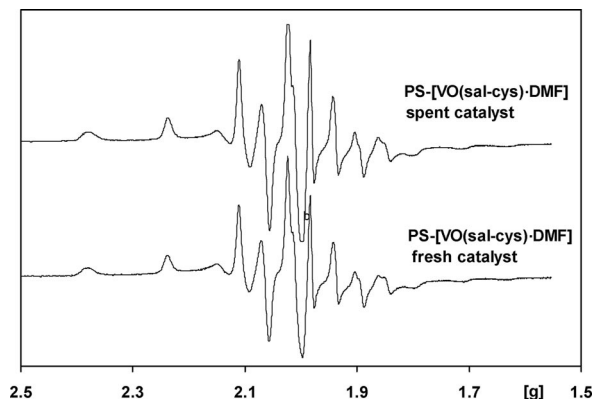

Figure 5. Powder EPR spectra of samples of the fresh and spent catalysts PS-[VO(sal-cys)·DMF] (**1**).

The EPR spectrum of DMSO solutions of the neat complex **2** was measured at 77 K. Immediately after dissolution the spectrum shows the presence of a broad band typical of aggregated molecules, possibly due to the presence of dimeric species (Figure 6). Such a dimeric structure has been confirmed for example for [VO(sal-ea)]$_2$ (H$_2$sal-ea is the Schiff base derived from salicylaldehyde and 2-aminoethanol) by a single-crystal X-ray diffraction study.[24] After some time under air the broad band progressively disappears and the final spectrum shows axial symmetry. The spin Hamiltonian parameters obtained by simulation of the experimental spectrum are: $g_\perp = 1.976$, $g_\parallel = 1.948$, $A_\perp = 59.0\times10^{-4}$ cm^{-1} and $A_\parallel = 165.0\times10^{-4}$ cm^{-1}. The value of $A_\parallel$ can be estimated ($A_\parallel^{est}$) using the additivity relationship proposed by Chasteen[27] with estimated accuracy of $\pm3\times10^{-4}$ cm^{-1}. This value can be correlated to the number and type of binding groups in the equatorial position, since each donor group has a specific contribution to the $A_\parallel$ and the sum of contributions of the four equatorial
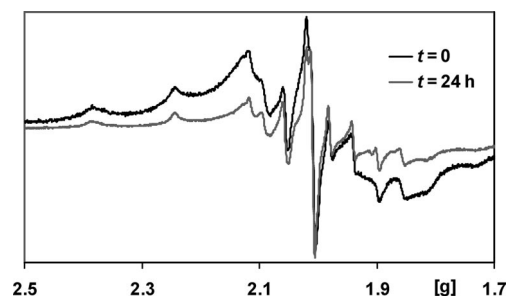

Figure 6. EPR spectra of frozen solutions (77 K) containing 5 mM of [VO(sal-eta)]$_2$ (**2**) dissolved in DMSO immediately after dissolution and after 24 h.

groups gives $A_\parallel^{est}$ that may be compared with the $A_\parallel$ observed. If we consider an equatorial binding mode involving [$O^-_{phenolate}$, N_{imine}, R–S$^-$, DMSO] the $A_\parallel^{est}$ = 153.9×10^{-4} cm^{-1},[28] which is too low. Therefore the coordination should involve [$O_{phenolate}$, N_{imine}, 2 × DMSO]$_{equatorial}$ and the thiolate group, if coordinated, should be in the axial position.

Catalytic Oxidative Amination of Styrene

Polymer-anchored complex, PS-[VO(sal-cys)·DMF] (**1**) catalyzes the oxidative amination of styrene with diethylamine, imidazole, and benzimidazole in the presence of oxygen and triethylamine, to give the corresponding enamines, Scheme 6. While HPLC gave an idea about percent conversion of styrene only, gas chromatography identified the two types of products formed, along with the percent conversion of styrene, and GC-MS confirmed their identities. Both types of products were finally separated by column liquid chromatography using chloroform as the eluent in all cases. Their ^{1}H NMR spectroscopic data, given in the experimental section, confirmed the formation of Markovnikov and anti-Markovnikov products. We did not observe any polymerization of styrene during the catalytic reaction. In order to optimize the catalytic activity of **1**, the following parameters were studied in detail considering diethylamine as a representative substrate:
(i) effect of the amount of amine (mol of amine per mol of styrene),
(ii) effect of the amount of catalyst (mol of catalyst per mol of styrene),
(iii) temperature of the reaction mixture.

Reactions were carried out at three different styrene to diethylamine molar ratios of 1:1, 1:1.5, and 1:2 using a fixed amount of styrene (1.04 g, 10 mmol), catalyst (0.030 g), and triethylamine (6.06 g, 60 mmol) in 20 mL of CH$_3$CN at 75 °C. Samples were periodically analyzed up to 4 h. As illustrated in Figure 7, a maximum of 32% conversion has been achieved after 4 h of reaction time at a styrene to amine molar ratio of 1:1. Increasing this ratio to 1:1.5 led to a conversion of ca. 45% while 1:2 molar ratios showed a maximum of ca. 73% conversion. In another experiment, three different catalyst loadings (viz. 0.020 g, 0.030 g, and

0.040 g) were considered at a styrene to amine ratio of 1:2 under the above reaction conditions, and the results are given in Figure 8. As can be seen in the figure, 0.020 g of catalyst gave only 29.5% conversion while 0.030 g and 0.040 g of catalyst loadings have shown a comparable conversion of 73 and 76%, respectively. Thus, 0.030 g of catalyst was found to be adequate to carry out the reaction for maximum production. The temperature of the reaction mixture has also influence on the performance of the catalyst. As shown in Figure 9, running the reaction at 75 °C gave a much better yield of the reaction products than at 50 or 65 °C.
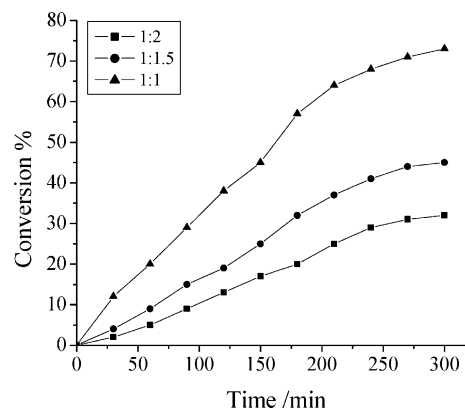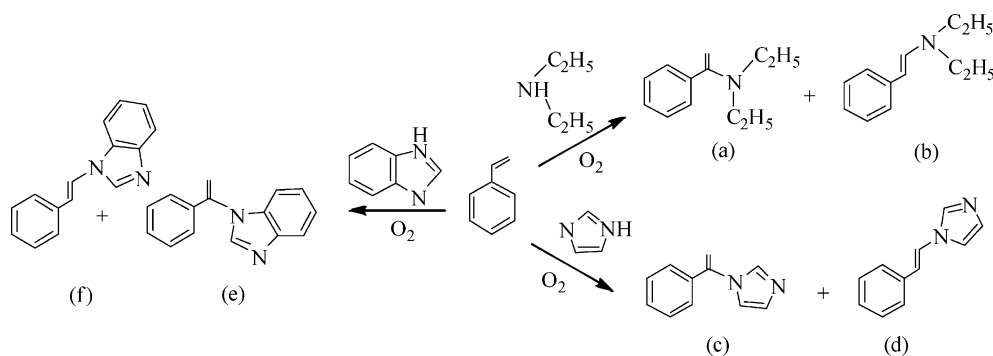

Figure 7. Effect of styrene to diethylamine ratio on the oxidative amination of styrene. Reaction conditions: styrene (1.04 g, 10 mmol), PS-[VO(sal-cys)·DMF] (0.030 g) and triethylamine (6.06 g, 60 mmol) in 20 mL of CH$_3$CN at 75 °C.

Under the optimized conditions, i.e. styrene (1.04 g, 10 mmol), catalyst PS-[VO(sal-cys)·DMF] (0.030 g), triethylamine (6.06 g, 60 mmol), CH$_3$CN (20 mL) and temperature (75 °C), the oxidative amination of styrene, catalyzed by **1**, with imidazole and benzimidazole (20 mmol each) has also been carried out, and the progress of the formation of aminated products as a function of time is presented in Figure 10. It is clear from the Figure that diethylamine gave a maximum of 73% conversion, followed by imidazole with 56%, and benzimidazole gave only 24% conversion. The enamines formed do not hydrolyze into the corresponding carbonyl and amine compounds under the influence of water produced during catalytic reactions. However, its

Scheme 6. a: *N*,*N*-Diethyl-1-phenylethenamine, b: *N*,*N*-diethyl-1,2-phenylethenamine, c: 1-(1-phenylvinyl)-1*H*-imidazole, d: 1-styryl-1*H*-imidazole, e: 1-(1-phenylvinyl)-1*H*-benzimidazole and f: 1-styryl-1*H*-benzimidazole.
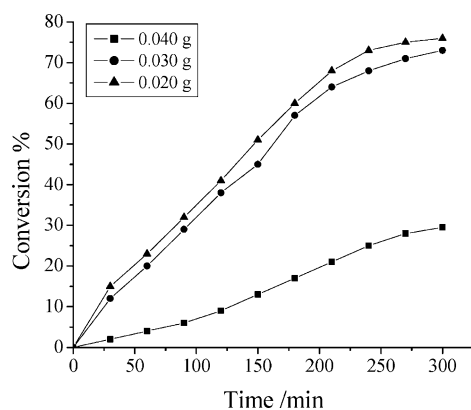
Figure 8. Effect of the amount of catalyst PS-[VO(sal-cys)·DMF] on the oxidative amination of styrene with diethylamine. Reaction conditions: styrene (1.04 g, 10 mmol), styrene/amine (1:2) and triethylamine (6.06 g, 60 mmol) in 20 mL of CH$_3$CN at 75 °C.
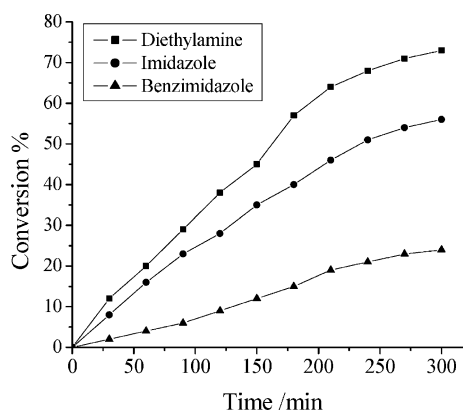

Figure 10. Comparison of the activity of PS-[VO(sal-cys)·DMF] for different substrates. Reaction conditions: styrene (1.04 g, 10 mmol), PS-[VO(sal-cys)·DMF] (0.030 g) and triethylamine (6.06 g, 60 mmol), secondary amine (20 mmol) in 20 mL of CH$_3$CN at 75 °C.
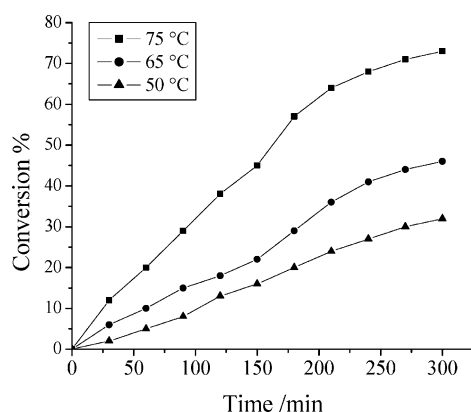

Figure 9. Effect of the temperature on the oxidative amination of styrene with diethylamine. Reaction conditions: styrene (1.04 g, 10 mmol), PS-[VO(sal-cys)·DMF] (0.030 g) and triethylamine (6.06 g, 60 mmol) in 20 mL of CH$_3$CN.

presence only slightly affected the conversion. The elimination of water from the reaction mixture by using dry molecular sieves (4 Å) improved the conversion by ca. 2%.

Table 4 presents data on conversion, turn over frequency (TOF) of the catalysts, and selectivity of the Markovnikov and anti-Markovnikov products obtained. It is clear from the Table that the selectivity of *N,N*-diethyl-1,2-phenylethenamine, 1-styryl-1*H*-imidazole, and 1-styryl-1*H*-benzimidazole, i.e. the yield of the anti-Markovnikov products (see Scheme 6), are higher than those of *N,N*-diethyl-1-phenylethenamine, 1-(1-phenylvinyl)-1*H*-imidazole, and 1-(1-phenylvinyl)-1*H*-benzimidazole, i.e. the Markovnikov

products. This can be rationalized taking into account the steric hindrance imposed by the secondary amine, which decreases the formation of the Markovnikov products. Thus, benzimidazole, having the highest steric hindrance, resulted in the formation of 1-(1-phenylvinyl)-1*H*-benzimidazole in lower yield. Within the anti-Markovnikov products the selectivity follows the order: 1-styryl-1*H*-benzimidazole (81%) > 1-styryl-1*H*-imidazole (74%) > *N,N*-diethyl-1,2-phenylethenamine (71%). This is again in accordance with the order of decreasing steric hindrance.

We have also tested the catalytic activity of the neat complex **2**, a close analogue of **1** in terms of coordination environment, in the oxidative amination of styrene taking the same mol concentration as used for **1**. Its performance for various aminated products after 4 h of reaction is also presented in Table 4. It is clear from the Table that the neat complex exhibits slightly lower conversion than the anchored analogue for all reactions. The improvement in the catalytic activity of the anchored complex may be due to uniform distribution of metal centers on the polymer matrix, and/or an increased availability of styrene molecules which may adsorb on the polymer, close to the catalyst. The carboxylate group on the α-position of nitrogen has no influence on the catalytic reaction as it is bound to the polymer.

The selectivity of the Markovnikov aminated products is slightly higher for the neat complex than for the anchored one. However, this effect is rather marginal and may be due to additional steric hindrance posed by polymeric support

Table 4. Conversion and reaction products using neat **2** and anchored **1** catalysts.

Entry	Catalyst		% Conversion	TOF [h^{-1}]	% Yield Markovnikov product	anti-Markovnikov product
1	**1**	diethylamine	73.2	39	28.8	71.2
2	**1**	imidazole	56.3	30	25.9	74.1
3	**1**	benzimidazole	24.1	13	18.9	81.1
4	**2**	diethylamine	65.3	21	32.6	67.4
5	**2**	imidazole	47.4	14	26.9	73.1
6	**2**	benzimidazole	21.3	7	20.7	79.3

to anchored catalyst which might restrict the Markovnikov product formation. The calculated turn-over frequency for all the reactions with anchored catalyst are higher than those carried out using the neat complex. Besides, its stability and recycle ability make the anchored catalyst better than the neat analogue.

Possible Routes to Amination

When carrying out catalytic reactions with Pt-, Pd-, Rh-, and Ru- etc. -based catalysts, Müller and Beller[1] suggested that a possible route for oxidative amination is through intermediate complex formation of styrene with the catalyst. This intermediate then couples with the amine to give another aminoalkyl intermediate complex, followed by oxidative cleavage of the M–C bond in the presence of O_2. As our catalytic system is based on an oxidovanadium-(IV) complex and no vanadium(IV)–styrene interaction is reported in the literature, we have explored this possibility by studying the interaction of the neat vanadium complex, $[VO(sal-eta)]_2$ with styrene and/or diethylamine by spectroscopic techniques: UV/Vis absorption and EPR.

UV/Vis Spectral Studies

We started by treating the neat vanadium complex, $[VO(sal-eta)]_2$ (2) with styrene in dichloromethane in the presence of a small amount of triethylamine, i.e. under the reaction conditions applied for oxidative amination, and monitored the resulting changes by electronic absorption spectroscopy. Thus, the addition of one drop of 0.5-molar styrene solution in CH_2Cl_2 (complex 2/styrene molar ratio of ca. 1:10) to 5 mL of ca. 10^{-4} molar solutions of 2 in dichloromethane resulted in the spectral changes with time presented in Figure 11 (a). The intensity of the 353 nm band slowly decreases after the addition of styrene, while the intensity of the 319 nm band increases. The band at 277 nm only gains intensity. The position and optical densities of the bands due to d-d transitions remain constant; therefore the main features of the coordination geometry around the vanadium center do not change much (cf. inset of part a of Figure 11). Rather similar spectral changes have also been observed when a solution of 2 in dichloromethane, also containing a small amount of triethylamine was treated with either diethylamine (complex 2/diethylamine molar ratio of ca. 1:10; Figure 11, b), or a mixture of styrene and diethylamine (Figure 11, c). However, visible changes in d-d bands have been observed on passing oxygen through a solution of 2 containing one drop of 0.5-molar styrene solution and a small amount of triethylamine in CH_2Cl_2 (complex 2/styrene molar ratio of ca. 1:10; Figure 11, d). Here, both d-d bands slowly disappear indicating the oxidation of oxidovanadium(IV) complex to an oxidovanadium(V) species in the presence of styrene. A similar
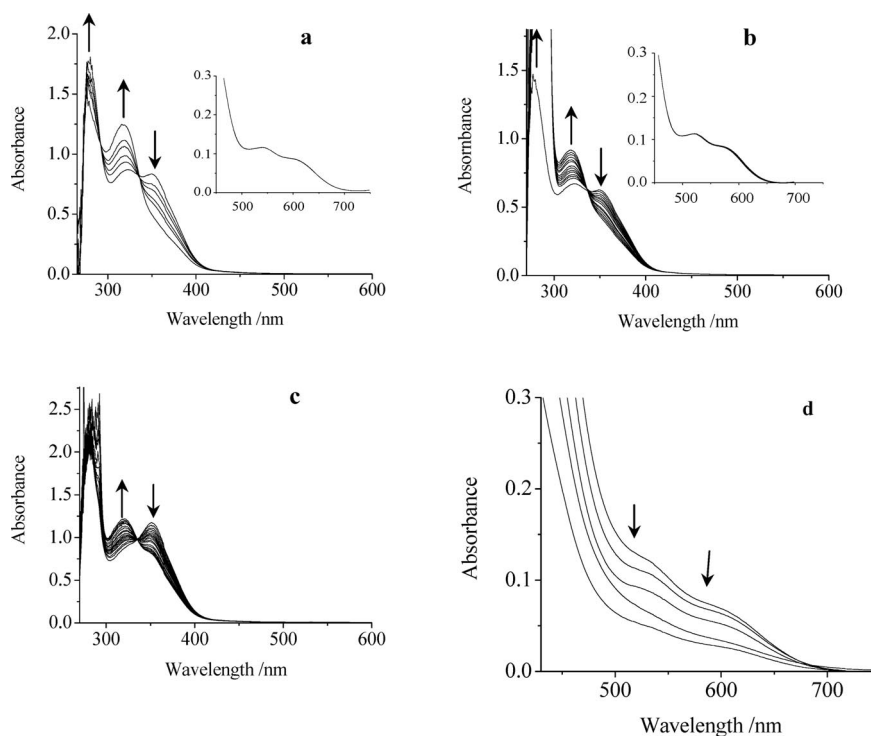

Figure 11. Change with time of the UV/Vis spectra of ca. 5 mL of a 10^{-4} M solution of $[VO(sal-eta)]_2$ (2) in dichloromethane, in the presence of a small amount of triethylamine, after the addition of: (a) one drop of 0.5-molar styrene solution (complex 2/styrene molar ratio of ca. 1:10), (b) one drop of 0.5-molar diethylamine solution (complex 2/diethylamine molar ratio of ca. 1:10), and (c) one drop of 0.5-molar styrene solution and one drop of 0.5-molar diethylamine solution (again complex 2: styrene: diethylamine molar ratio of ca. 1:10:10) and (d) one drop of 0.5-molar styrene solution (complex 2/styrene molar ratio of ca. 1:10) in the presence of oxygen. Spectra were recorded in 15 min intervals. With triethylamine no such changes were observed in the absorption spectra of solutions of 2.

observation has also been observed on passing oxygen through a solution of **2** containing one drop of 0.5-molar diethylamine solution and a small amount of triethylamine in CH₂Cl₂ (complex **2**/diethylamine molar ratio of ca. 1:10). It is important to note that passing of oxygen for days through a CH₂Cl₂ solution of **2** had no effect on the visible spectra.

The interpretation of the changes shown in Figure 11 is not straightforward. However, the changes described above hint towards the participation of styrene or diethylamine in the process of oxidation of oxidovanadium(IV) to oxidovanadium(V) in the presence of oxygen, followed by elimination of the aminated product(s). It is possible that the catalytic and redox processes operating involve coordinated styrene and/or amine. However, it is not possible at this stage to comment further on the exact nature of these processes and we are pursuing further theoretical and experimental studies in this field. With other metal complexes similar types of interactions have been discussed in the literature.[1]

EPR Spectral Studies

In order to find evidence for the intermediate species formed during the catalytic cycle, the neat complex [VO-(sal-eta)]₂ was dissolved in DMSO containing 2 equiv. of triethylamine and different amounts of styrene and/or diethylamine were added. Only after addition of ca. 10 equiv. of styrene is a new species clearly detected by EPR, this being shown in Figures 12 and 13. Figure 13 shows the

high-field region of the EPR spectra of frozen solutions containing 5 mM of [VO(sal-eta)]₂ and 1, 2, 3, and 10 molar equivalents of the substrates. Upon addition of styrene, diethylamine or both, the broad band indicative of the presence of the dimeric form of [VO(sal-eta)]₂ decreases its intensity, and a monomeric form corresponding to [VO-(sal-eta)], possibly with a binding mode involving [$O_{phenolate}$, N_{imine}, 2 × DMSO]$_{equatorial}$, becomes the main species detected. In the solutions where diethylamine is added (Figure 13, b), no change in the EPR spectra was detected that may support its equatorial coordination. However, its coordination *trans* to the oxo-oxygen atom cannot be ruled out.
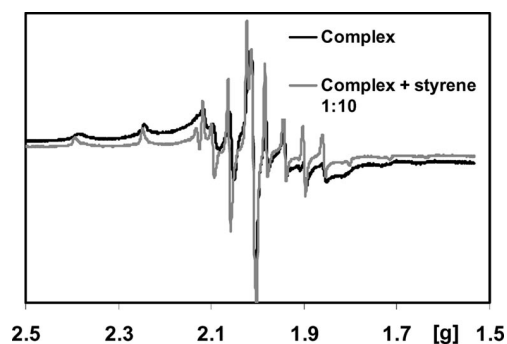

Figure 12. EPR spectra of frozen solutions containing the neat complex **2** (5 mM) dissolved in DMSO, with and without 10 equiv. of styrene. The presence of a new species is clearly seen in the high- and low-field regions of the spectrum printed in gray.
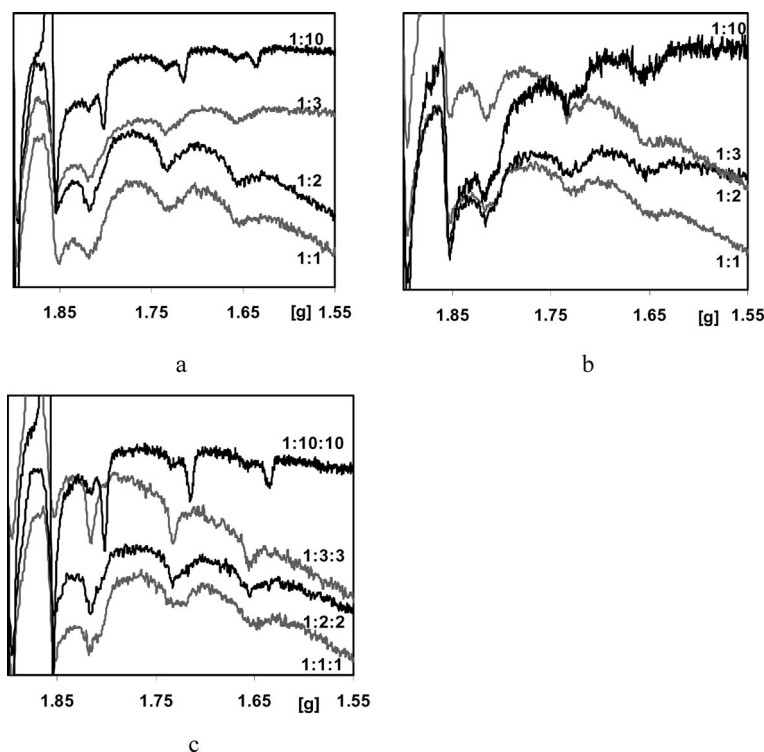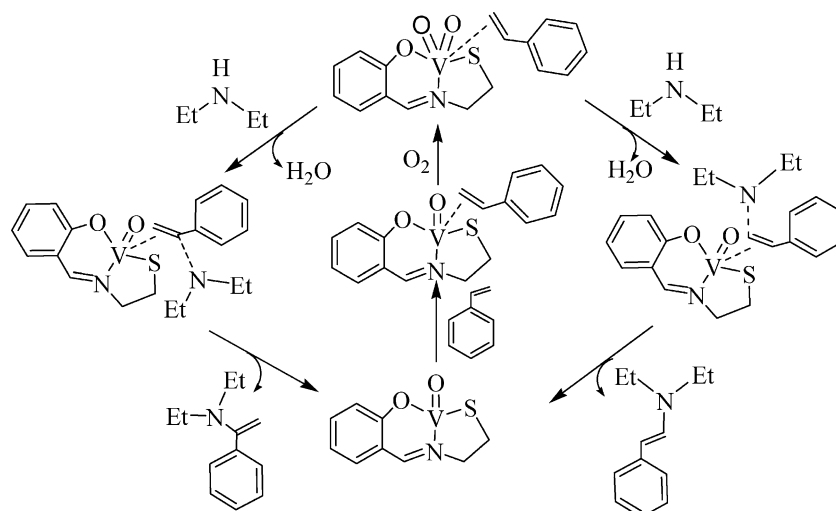

Figure 13. High-field region of the EPR spectra of frozen DMSO solutions (77 K) containing 5 mM of complex **2** and 1, 2, 3, or 10 equiv. of styrene and/or diethylamine. (a) Complex **2** + styrene, (b) complex **2** + diethylamine, (c) complex **2** + styrene + diethylamine.

Scheme 7. Proposed overall mechanism for the oxidative amination of styrene. Only a schematic representation of [VO(sal-eta)]$_2$ (**2**) is shown.

The parameters for the new species formed (gray spectrum in Figure 12) are totally different from those of the complex in the absence of such an excess of styrene, and correspond to a higher $A_\parallel$ value. The spin Hamiltonian parameters were obtained by simulation: $g_\perp = 1.979$, $g_\parallel = 1.945$, $A_\perp = 60.4 \times 10^{-4}$ cm^{-1}, and $A_\parallel = 168.9 \times 10^{-4}$ cm^{-1}. These results clearly show that only in the presence of styrene a clear change occurs in the EPR spectra, resulting from a change in the coordination environment of the vanadium center, and these changes can only be reasonably explained by assuming the coordination of styrene. To the best of our knowledge there is no data in the literature for the contribution of a coordinated olefin to $A_\parallel$. This evidence for the coordination of styrene to vanadium supports the mechanism for the reaction proposed in Scheme 7.

Proposed Mechanism of the Catalytic Reaction

On the basis of the spectroscopic (EPR and electronic) results, it is reasonable to propose that the oxidovanadium-(IV) activates the olefin via complex formation possibly through π-bonding of the alkene group followed by its oxidation to an oxidovanadium(V) species. Complex formation of olefin through π-bonding causes partial shifting of the electron density from the double bond to the empty d-orbital of the vanadium followed by polarization of the double bond. While the dioxo complex interacts with secondary amine through hydrogen bonding and come close to styrene, the polarization facilitates the nucleophilic attack of secondary amines to styrene. Because of the close proximity of two hydrogen atoms and the oxygen of the oxo group of the dioxidovanadium(V) species, the reductive removal of water and formation of an oxidovanadium(IV) intermediate species may result immediately. This process is fast and is not observable when all reagents are taken together and monitored by either EPR or electronic absorption spectroscopy.

Whether the secondary amine coordinates in an axial position to the vanadium center is not clear. Assuming this intermediate indeed forms, the selectivity could eventually be explained by a higher stability of the conformer that would lead to the anti-Markovnikov product. Alternatively, the selectivity may be more easily explained on the basis of the aminoalkyloxidovanadium species. Two distinct such intermediates may form: one corresponding to the Markovnikov product, and the other corresponding to the anti-Markovnikov product, the latter involving less steric hindrance, thereby being favored.

The formation of the final product is obtained by elimination of aminated species through cleavage of the vanadium–carbon bond. Because of the steric crowd present on the secondary amine, the formation of the second intermediate species becomes more favorable and hence the yield of the second product (see parts b, d, or f in Scheme 6) is higher than the yield of the first product (see parts a, c, or e in Scheme 6). The whole mechanism is illustrated in Scheme 7. It is clear from the mechanism that the steric crowd present on the secondary amine will direct the final product. Thus, the anti-Markovnikov product will be favored over the Markovnikov product. Our experimental results (vide supra) also support this mechanism.

Conclusions

A polymer-anchored oxidovanadium(IV) complex, PS-[VO(sal-cys)·DMF] of the Schiff base derived from the reaction of salicylaldehyde and L-cysteine (H$_2$sal-cys) has been prepared and characterized. The catalytic activity of PS-[VO(sal-cys)·DMF] for the oxidative amination of styrene with secondary amines such as diethylamine, imidazole, and benzimidazole in mild basic conditions gave a mixture of two aminated products in good yields. The steric hindrance present on the secondary amine directs the formation of the final product and the anti-Markovnikov products have been

obtained in major yield. The corresponding neat complex, [VO(sal-eta)]$_2$ (H$_2$sal-eta is the Schiff base derived from salicylaldehyde and 2-aminoethanethiol) has also been prepared. The catalytic activity of the neat complex has also been found to be good. This study presents the first report of an oxidovanadium(IV) complex for oxidative aminations. The formation of possible intermediates during catalytic action have been explored by titrating solutions of the neat complex [VO(sal-eta)]$_2$ with styrene, diethylamine, or a mixture of styrene and diethylamine in the presence of a small amount of triethylamine, following the titrations by EPR spectroscopy. The EPR data gave evidence for the coordination of styrene to vanadium, therefore supporting a mechanism for catalysis involving activation of the olefin via complex formation followed by the attack by the amine. UV/Vis experiments in the presence of O$_2$ indicate the formation of a dioxidovanadium(V) species, suggesting the participation of this species in the final redox steps that lead to the formation of the enamine products.

Experimental Section

Materials and Methods: Analytical reagent grade 2-aminoethanethiol hydrochloride (Aldrich Chemicals Co., USA), L-cysteine, imidazole, benzimidazole (S. D. Fine Chemicals, India), styrene (Acros Organics, USA), V$_2$O$_5$, (Loba Chemie, India), acetylacetone (E. Merck, India), aqueous 30% H$_2$O$_2$, salicylaldehyde (Ranbaxy, India), and other chemicals were used as obtained. [VO(acac)$_2$][29] and H$_2$sal-cys[30] were prepared according to the methods reported in the literature.

Physical and Spectroscopic Studies: Elemental analyses of the ligands and complexes were obtained with an Elementar model Vario-EL-III. IR spectra were recorded as KBr pellets with a Nicolet NEXUS Aligent 1100 FT-IR spectrometer. Electronic spectra of polymer-anchored compounds were recorded in Nujol with a Shimadzu 1601 UV/Vis spectrophotometer by layering the sample mull inside of one of the cuvettes while keeping the other one layered with Nujol as reference. Other ligands and complexes were recorded in methanol. ^{1}H NMR spectra were obtained with a Bruker 500 MHz spectrometer in [D$_6$]DMSO. The EPR spectra were recorded with a Bruker ESP 300E X-band spectrometer. For the polymer-anchored complex samples the spectra were measured at room temperature and for the neat complex samples in DMSO the EPR spectra were measured at 77 K (with glasses made by freezing the solutions in liquid nitrogen). The spin Hamiltonian parameters were obtained by simulation of the spectra with the computer program of Rockenbauer and Korecz.[31] The magnetic susceptibility of oxidovanadium(IV) complex was measured at 298 K with a Vibrating Sample Magnetometer model 155, using nickel as the standard. Diamagnetic corrections were carried out using Pascal's increments.[32] Thermogravimetric analyses of the complexes were carried out using a TG Stanton Redcroft STA 780 under an oxygen atmosphere. Scanning Electron Micrographs (SEM) of catalysts were recorded with a Leo instrument model 435 VP. The samples were coated with a thin film of gold to prevent surface changing and to protect the surface material from thermal damage by the electron beam.

Synthesis of Ligands and Complexes

H$_2$sal-cys (I): Ligand H$_2$sal-cys was prepared as reported in the literature.[30] Yield 70%. ^{1}H NMR ([D$_6$]DMSO): δ = 4.22 (br., 1 H, phenolic OH), 8.09 (d, 1 H, aromatic), 7.06–7.34 (m, 1 H, aromatic), 6.76–6.81 (m, 2 H, aromatic), 5.65, 5.84 (s, 1 H, -CH=N-, geometrical isomers), 3.21, 3.34 (br., 1 H each, -CH$_2$) ppm. ^{13}C NMR ([D$_6$]DMSO): δ = 173.4 (carboxylic), 156.4 (azomethine), 155.1 (phenolic), 129.5, 128.6, 119.5, 119.2, 116.2 (aromatic), 65.2, 38.6 (alkyl chain) ppm. IR and ^{1}H NMR spectroscopic data match well with the literature values.

PS-H$_2$sal-cys (II): Chloromethylated polystyrene (4.0 g) was suspended in DMF (30 mL) for 2 h. A solution of H$_2$sal-cys (13.44 g, 60 mmol) dissolved in 40 mL of DMF was added to the above suspension followed by triethylamine (5.05 g, 50 mmol) in ethyl acetate (50 mL). The reaction mixture was heated at 90 °C for 20 h with mechanical stirring in an oil bath. After cooling to room temperature, the yellow resin beads were separated by filtration, washed thoroughly with hot DMF followed by hot methanol, and dried in an air oven at 120 °C.

H$_2$sal-eta (III): Ligand **III** was prepared following the literature procedure. A solution of 2-aminoethanethiol hydrochloride (1.13 g, 10 mmol) dissolved in methanol (15 mL) was treated with KOH (0.56 g, 10 mmol) and stirred for 1 h. After filtration, it was added to a solution of salicylaldehyde (1.22 g, 10 mmol) dissolved in 10 mL of methanol and stirred for 3 h. After reducing the volume of the solvent to ca. 10 mL, it was kept in a refrigerator where a yellow solid slowly precipitated over 1 week. This was filtered, washed with a small amount of cold methanol and dried in vacuo; yield 82%. ^{1}H NMR ([D$_6$]DMSO): δ = 13.31 (br., 1 H, phenolic-OH), 8.57 (s, 1 H, -CH=N-), 7.44–6.87 (m, 4 H, aromatic), 3.88 (s, 2 H, -CH$_2$-), 3.08 (s, 2 H, -CH$_2$-) ppm. ^{13}C NMR ([D$_6$]DMSO): δ = 167.4 (azomethine), 160.9 (phenolic), 132.9, 132.2, 119.3, 119.1, 116.9 (aromatic), 57.2, 38.9 (alkyl chain) ppm.

PS-[VO(sal-cys)·DMF] (1): The polymer-anchored ligand PS-H$_2$sal-cys (2.0 g) was allowed to swell in DMF (20 mL) for 2 h and to this a solution of [VO(acac)$_2$] (5.30 g, 20 mmol) in DMF (50 mL) was added and the reaction mixture was heated at ca. 90 °C in an oil bath for 15 h with slow mechanical stirring. The blackish green beads of PS-[VO(sal-cys)·DMF] were filtered off, washed with hot DMF followed by hot methanol, and dried in an air oven at 120 °C.

[VO(sal-eta)]$_2$ (2): A solution of H$_2$sal-eta (0.36 g, 2 mmol) in acetonitrile (20 mL) was stirred with [VO(acac)$_2$] (0.53 g, 2 mmol) dissolved in acetonitrile (20 mL) for 4 h. The precipitated green solid of [VO(sal-eta)]$_2$ was filtered off, washed with acetonitrile, and dried in vacuo; yield 65%.

Oxidative Amination of Styrene: The oxidative amination of styrene was carried out in a 50-mL two-necked reaction flask fitted with a septum and water circulated condenser. The polymer-anchored complex was allowed to swell in acetonitrile for 2 h prior to use in each experiment. In a typical reaction, styrene (2.08 g, 20 mmol), 40 mmol secondary amine (diethylamine, 2.92 g; imidazole, 2.72 g or benzimidazole 4.81 g) and triethylamine (6.06 g, 60 mmol) were mixed in 20 mL of acetonitrile and the reaction mixture was heated at 75 °C with the continuous bubbling of oxygen through a syringe. Catalyst, PS-[VO(sal-cys)·DMF] (0.030 g) was added to the reaction mixture and stirred for 4 h. The progress of the reaction was monitored by withdrawing small amounts of the reaction mixture at different time intervals and analyzing them quantitatively by HPLC [with an Agilent 1100 series model equipped with a Hypersil® BDS C$_{18}$ (250 × 4.6 mm, 5 µ) column (30:70, water/acetonitrile)]. Finally products were identified quantitatively using a Thermoelectron gas-chromatograph with an HP-1 capillary column (30 m × 0.25 mm × 0.25 µm) and FID detector. The identities of the products were confirmed by GC-MS (Perkin–Elmer, Clarus 500). The effect of various parameters such as temperature, amount of

secondary amine and catalyst were studied to obtain suitable reaction conditions for the best performance of the catalyst.

Characterization of Aminated Products

Aminated Products with Diethylamine: (i) ^{1}H NMR ([D$_6$]DMSO) (*N,N*-diethyl-2-phenylethanamine): δ = 7.5 (d, 1 H, =N-CH=), 7.47–7.26 (m, 5 H, aromatic), 5.37 (d, 1 H, -CH=), 3.51 (q, 4 H, -CH$_2$-), 0.99 (t, 6 H, CH$_3$) ppm. (ii) ^{1}H NMR ([D$_6$]DMSO) (*N,N*-diethyl-1-phenylethanamine): δ = 7.48–7.26 (m, 5 H, aromatic), 4.63, 4.0 (d, 1 H each, =CH-), 3.34 (q, 4 H, -CH$_2$-), 0.99 (t, 6 H, -CH$_3$) ppm.

Aminated Products with Imidazole: (i) ^{1}H NMR ([D$_6$]DMSO) (1-styryl-1*H*-imidazole): δ = 8.09 (s, 1 H, imidazole ring =CH-), 7.71–7.26 (m, 5 H, aromatic), 7.35 (d, 2 H, imidazole ring-CH=CH-), 6.37 (d, 1 H, =CH-), 5.64 (d, 1 H, =N-CH=) ppm. (ii) ^{1}H NMR ([D$_6$]DMSO) [1-(1-phenylvinyl)-1*H*-imidazole]: δ = 8.10 (s, 1 H, imidazole ring =CH-), 7.71 (d, 2 H, imidazole ring-CH=CH-), 7.47–7.07 (m, 5 H, aromatic), 5.63, 5.25 (d, 1 H each, =CH-) ppm.

Aminated Products with Benzimidazole: (i) ^{1}H NMR ([D$_6$]DMSO) (1-styryl-1*H*-benzimidazole): δ = 8.28 (s, benzimidazole ring =CH-), 7.69–7.23 (m, 9 H, aromatic), 6.21 (d, 1 H, =CH-), 5.84 (d, 1 H, =N-CH=) ppm. (ii) ^{1}H NMR ([D$_6$]DMSO) [1-(1-phenylvinyl)-1*H*-benzimidazole]: δ = 8.11 (s, benzimidazole ring =CH-), 7.47–7.26 (m, 9 H, aromatic), 6.28, 5.63 (d, 1 H each, =CH-) ppm.

Acknowledgments

[1] T. E. Müller, M. Beller, *Chem. Rev.* **1998**, *98*, 675–703.
[2] H. Trauthwein, A. Tillack, M. Beller, *Chem. Commun.* **1999**, 2029–2030.
[3] M. Kawatsura, J. F. Hartwig, *J. Am. Chem. Soc.* **2000**, *122*, 9546–9547.
[4] U. Nettekoven, J. F. Hartwig, *J. Am. Chem. Soc.* **2002**, *124*, 166–1167.
[5] M. R. Gagne, S. P. Nolan, T. J. Marks, *Organometallics* **1990**, *9*, 1716–1718.
[6] S. Tian, V. M. Arredondo, C. L. Stern, T. J. Marks, *Organometallics* **1999**, *18*, 2568–2570.
[7] J. F. Hartwig, *Pure Appl. Chem.* **2004**, *76*, 507–516.
[8] T. Kondo, T. Okada, T. Mitsudo, *J. Am. Chem. Soc.* **2002**, *124*, 186–187.
[9] M. Beller, H. Trauthwein, M. Eichberger, C. Breindl, T. E. Müller, A. Zapf, *J. Organomet. Chem.* **1998**, *566*, 277–285.
[10] J. L. Brice, J. E. Harang, V. I. Timokhin, N. R. Anastasi, S. S. Stahl, *J. Am. Chem. Soc.* **2005**, *127*, 2868–2869.
[11] V. N. Srinivasarao, S. K. Talluri, G. Shyla, S. A. Rumugam, *Tetrahedron Lett.* **2007**, *48*, 65–68.
[12] S. R. Fix, J. L. Brice, S. S. Stahl, *Angew. Chem. Int. Ed.* **2002**, *41*, 164–166.
[13] V. V. Goryunenko, A. V. Gulevskaya, A. F. Pozharskii, *Russ. Chem. Bull., Int. Ed.* **2004**, *53*, 846–852.
[14] A. Tillack, H. Trauthwein, C. G. Hartung, M. Eichberger, S. Pitter, A. Jansen, M. Beller, *Monatsh. Chem.* **2000**, *131*, 1327–1334.
[15] M. Beller, H. Trauthwein, M. Eichberger, C. Breindl, T. E. Müller, *Eur. J. Inorg. Chem.* **1999**, 1121–1132.
[16] M. Beller, H. Trauthwein, M. Eichberger, C. Breindl, J. Herwig, T. E. Müller, O. R. Thiel, *Chem. Eur. J.* **1999**, *5*, 1306–1319.
[17] F. Ragaini, T. Longo, S. Cenini, *J. Mol. Catal. A* **1996**, *110*, L171 –L175.
[18] J.-J. Brunet, D. Neibecker, K. Philippot, *Tetrahedron Lett.* **1993**, *34*, 3877–3880.
[19] T. Hosokawa, M. Takano, Y. Kuroki, S.-I. Murahashi, *Tetrahedron Lett.* **1992**, *33*, 6643–6646.
[20] J. J. Bozell, L. S. Hegedus, *J. Org. Chem.* **1981**, *46*, 2561–2563.
[21] M. J. Gaunt, J. B. Spencer, *Org. Lett.* **2001**, *3*, 25–28.
[22] A. Syamal, K. S. Kale, *Inorg. Chem.* **1979**, *18*, 992–995.
[23] A. Syamal, K. S. Kale, *Indian J. Chem.* **1980**, *19A*, 225–228.
[24] C. J. Carrano, C. M. Nunn, R. Quan, J. A. Bonadies, V. L. Pecoraro, *Inorg. Chem.* **1990**, *29*, 944–951.
[25] M. R. Maurya, U. Kumar, P. Manikandan, *Dalton Trans.* **2006**, 3561–3575.
[26] A. Syamal, O. P. Singhal, *J. Inorg. Nucl. Chem.* **1981**, *43*, 2821–2825.
[27] N. D. Chasteen in *Biological Magnetic Resonance* (Eds.: J. Lawrence, L. J. Berliner, J. Reuben), Plenum, New York, **1981**, Ch. 2, p. 53–119.
[28] C. R. Cornman, E. P. Zovinka, Y. D. Boyajian, K. M. Geiser-Bush, P. D. Boyle, P. Singh, *Inorg. Chem.* **1995**, *34*, 4213–4219.
[29] R. A. Rowe, M. M. Jones, *Inorg. Synth.* **1957**, *5*, 113–116.
[30] M. R. A. Pillai, K. Kothari, S. Banerjee, G. Samuel, M. Suresh, H. D. Sharma, S. Jurisson, *Nucl. Med. Biol.* **1999**, *26*, 555–561.
[31] A. Rockenbauer, L. Korecz, *Appl. Magn. Reson.* **1996**, *10*, 29–43.
[32] R. L. Dutta and A. Syamal, *Elements of Magnetochemistry*, 2nd ed., Affiliated East-West Press, New Delhi, **1993**, p. 8.